6.9 THE MECHANISM FOR THE MAINTENANCE OF DECADAL SST ANOMALIES IN THE MIDLATITUDE NORTH PACIFIC

Takashi Mochizuki * and Hideji Kida
Kyoto University, Kyoto, Japan

1. INTRODUCTION

The spatial structure of the decadal SST variations over the North Pacific is generally characterized by the cool (warm) anomalies spreading over the midlatitude in contrast with the warm (cool) anomalies in the tropics and along the western coast of North America. However, investigating more detailed spatial structures SST in the midlatitude, the strong decadal variations appear in the northern region (39N-49N, 165E-155W) and the southern region (25N-35N, 175E-145W) (Fig.1; Nakamura et al. 1997).

Over the midlatitude North Pacific, some previous studies showed that the heat flux anomalies at the sea surface in winter would maintain the decadal SST anomalies (e.g., Barsugli and Battisti 1998; Saravanan 1998). In addition, a few studies pointed out that the vertical mixing anomaly in autumn would also play an important role in maintaining the decadal SST anomalies (e.g., Miller et al. 1994; Deser et al. 1996). It is however still uncertain whether or not these mechanisms could explain the maintenance of the decadal SST variations with the detailed spatial structures. It remains controversial which process is the most important to maintain the decadal SST anomalies. In this study the monthly variations and the mechanisms for the maintenance of decadal SST anomalies are discussed individually in the northern region and in the southern region.

2. DATA

The datasets used in this study are monthly mean global data of SST at $2^\circ \times 2^\circ$ (latitude×longitude) grids by the Japan Meteorological Agency (JMA), 1000hPa geopotential height at $2.5^\circ \times 2.5^\circ$ grids and many kinds of fluxes (wind stress, sensible heat flux, latent heat flux and net radiation flux at the surface) at T62 gaussian grids by the National Centers for Environmental Prediction/National Center for Atmospheric Research (NCEP/NCAR) reanalysis dataset, during 1950-97. Five-year running means in each month (averaging at the same five months during five years) are applied to these datasets in order to remove the ENSO components. Monthly climatology data of subsurface ocean properties (mixed layer depth, water temperature and salinity) from the World Ocean Atlas 1994 (WOA94) are also used.

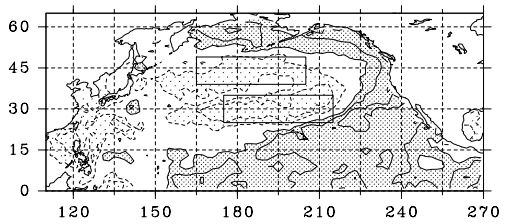

Fig. 1. Heterogeneous correlation pattern of global SST for the first SVD mode in winter (December - February). The contour interval is 0.25. Solid (dashed) lines represent positive (negative) value, and heavy (light) shaded regions denote areas larger than 0.25 (smaller than -0.25). Two rectangles represent the northern region (39N-49N, 165E-155W) and the southern region (25N-35N, 175E-145W).

3. DECADAL VARIATION OVER THE NORTH PACIFIC

We applied the singular value decomposition (SVD) analysis to North Pacific SST data and northern hemisphere 1000hPa geopotential height data to obtain coupled dominant decadal variation. Although heterogeneous correlation pattern of global SST (Fig.1) and its time coefficient (Fig.2) for the first SVD mode in winter (December - February) are similar to the decadal variation described in many previous studies, more detailed spatial structures are perceived in the midlatitude. The strongest decadal SST variations appear separately in the northern region (39N-49N, 165E-155W) and the southern region (25N-35N, 175E-145W).

Next, we applied SVD analysis to northern region SST (southern region SST) data and northern Hemisphere 1000hPa geopotential height data, to obtain coupled dominant decadal variations in the northern region (the southern region). For the first SVD mode in winter, the time coefficient of the northern region SST is different from that of the southern region SST (Fig.2). The dominant decadal variation of

* *Corresponding author address*: Takashi Mochizuki, Department of Geophysics, Graduate School of Science, Kyoto University, Kyoto 606-8502, Japan. E-mail: motizuki@kugi.kyoto-u.ac.jp

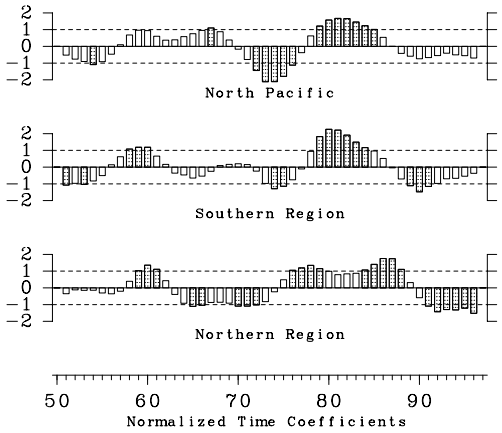

Fig. 2. The normalized time coefficients for the first SVD mode in winter (December - February) between northern Hemisphere 1000hPa geopotential height and North Pacific SST (upper), southern region SST (middle), and northern region SST (lower), respectively. Heavy shaded bars denote years defined as the DC+ (DC−) category, when the temporal coefficient deviates more than the one standard deviation in positive (negative) sign.

the northern region SST is characterized as the well-known late 1970s climate regime shift, while that of the southern region SST is regarded as decadal variation with periods of almost 10 years superimposed on the interdecadal variation with periods of 20-30 years. These results imply that the dominant decadal variations and the mechanisms of them could be different between in the northern region and the southern region.

4. MONTHLY VARIATIONS OF DECADAL SST TENDENCY ANOMALY

We examined the monthly variations of SST tendency, which is calculated as $[SST(t_{i+1}) - SST(t_{i-1})]/2$ $(K \cdot month^{-1})$ in the i-th month, to clarify the months when the decadal SST anomalies are maintained. In each region we defined the DC+ (DC−) category as years when the temporal coefficient of the first SVD mode deviates more than the one standard deviation in positive (negative) sign, and then calculated the composite value (the average in DC+ minus the average in DC−) of SST tendency every month.

The composite value of SST tendency becomes notable in the southern region during October - December, and in the northern region during November - January (Fig.3). And more, the year-to-year time series of SST tendency anomalies averaged during

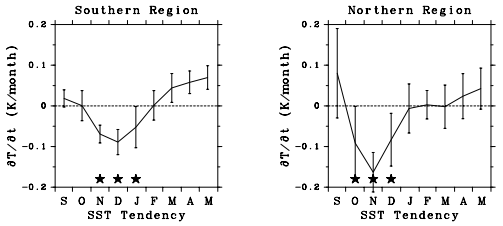

Fig. 3. The monthly variations during September - May of the composite value (the average in DC+ minus the average in DC−) of SST tendency in the southern region (left) and the northern region (right). Marked with stars (⋆) are the months when the composite value is notable and hence the decadal SST anomalies would be fairly maintained.

these months are well correlated with the time coefficients for the first SVD mode in each region (Fig.4). Hence, the decadal SST anomalies are maintained in the southern region during October - December and in the northern region during November - January.

5. HEAT BUDGET ANALYSIS FOR OCEAN MIXED LAYER

Toward understanding the mechanisms for the maintenance of decadal SST anomalies, we carried out the heat budget analysis for the ocean mixed layer and clarified dominant terms in the temperature equation.

The perturbation temperature equation for the ocean mixed layer, in which the perturbation of horizontal diffusion is assumed to be negligible, is written as

$$\frac{\partial T}{\partial t} + \mathbf{u} \cdot \nabla T + \frac{w \Delta T}{\overline{h}} + \frac{1}{\overline{h}} \frac{Q_{net}}{\rho_o c} = 0, \qquad (1)$$

where $\overline{h}$ is monthly climatology of ocean mixed layer depth in each grid point. $\partial T/\partial t$ represents temperature tendency anomaly assumed to be equal to SST tendency anomaly. $\mathbf{u} \cdot \nabla T$ represents horizontal temperature transport anomaly, where ∇T is horizontal temperature gradient assumed to be equal to SST gradient. The horizontal current, $\mathbf{u}$, is divided into two components, that is, geostrophic and Ekman parts. The geostrophic current velocity ($\mathbf{u}_g$) was calculated by upward integration from the 1000-m depth where $\mathbf{u}_g$ is assumed to be zero, using the climatological salinity and the water temperature data which is assumed to fluctuate only in the ocean mixed layer at the same magnitude as SST above. Although this is a rough estimate, the deviation scale can be grossly described. The Ekman

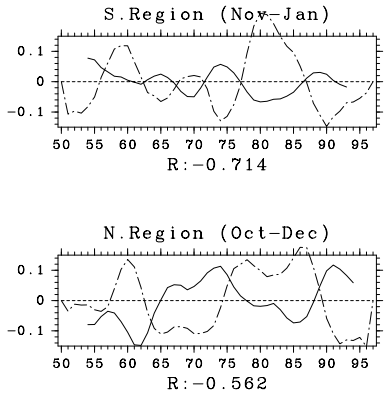

Fig. 4. The year-to-year variations of SST tendency anomalies (solid line) and time coefficients for the first SVD mode (dashed-dotted line), averaged during November - January in the southern region (upper), and during October - December in the northern region (lower). The unit for the SST tendency anomalies is $K \cdot month^{-1}$. Time coefficients are divided by the tenfold standard deviation. R represents the correlation coefficient between the time series of SST tendency anomalies and time coefficients for the first SVD mode.

current velocity ($\mathbf{u}_e$) was estimated as $(\tau \times \mathbf{k})/\rho_\circ f_\circ \overline{h}$, where τ, $\mathbf{k}$, $\rho_\circ$ and $f_\circ$ are the wind stress at the sea surface, the upward unit vector, the coriolis parameter and the constant density of sea water, respectively. Table1 shows the standard deviations of the temperature transport anomalies by geostrophic and Ekman advection, divided into two directions (zonal and meridional parts). Since meridional Ekman temperature transport ($v_e\ \partial T/\partial y$) is much stronger than any other component and is well correlated with the time coefficients for the first SVD mode (not shown), $\mathbf{u} \cdot \nabla T$ can be considered to equal $v_e\ \partial T/\partial y$. $w\Delta T/\overline{h}$ represents vertical temperature transport anomaly, which we estimated as a residual term. $Q_{net}/\rho_\circ c\overline{h}$ represents the total heat flux (the sum of sensible heat flux, latent heat flux and net radiation fluxes) anomaly at the sea surface, where c is the constant specific heat of seawater.

Figures 5 and 6 show the monthly variations of the composite value for the heat loss of ocean mixed layer by meridional Ekman advection and total heat flux at the sea surface, respectively. In the southern region, the decadal SST tendency anomaly balance only with the heat loss by meridional Ekman advection anomaly during November - January. In the northern region, the heat loss by the sum of meridional Ekman advection anomaly and total heat flux anomaly at the sea surface balance with the SST tendency anomaly during October - December. And the

	S. Region (Nov-Jan)	N. Region (Oct-Dec)
$u_g\ \partial T/\partial x$	410	764
$v_g\ \partial T/\partial y$	271	387
$u_e\ \partial T/\partial x$	105	249
$v_e\ \partial T/\partial y$	4478	4704
	$\times 10^{-5}(K \cdot month^{-1})$	

Table 1. The standard deviations of the zonal and meridional temperature transport anomalies by geostrophic current ($\mathbf{u}_g$) and Ekman current ($\mathbf{u}_e$), averaged during November - January in the southern region and during October - December in the northern region.

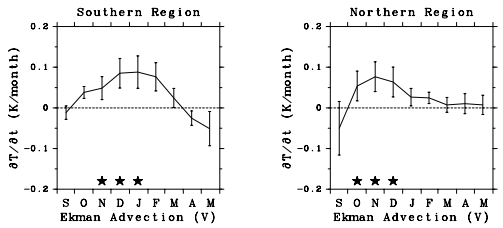

Fig. 5. Same as Fig.3, except for the composite value of the heat loss by meridional Ekman advection.

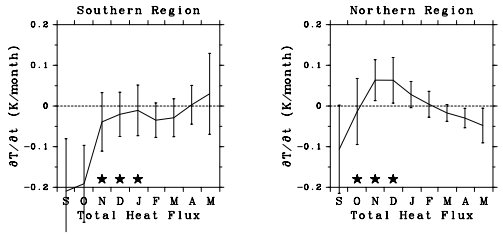

Fig. 6. Same as Fig.3, except for the composite value of the heat loss by total heat flux at the sea surface.

heat loss by meridional Ekman advection anomaly is the strongest at the southern part (39N-43N) far from the continents, while the heat loss by total heat flux anomaly is the strongest at the northern part (45N-49N) near the continents (Fig.7). The vertical temperature transport, estimated as a residual term, is very small (not shown).

The decadal variation of ocean mixed layer depth, h, is ignored in this study. Miller et al. (1994) and Deser et al. (1996) concluded that vertical mixing is one of the most important processes for changing the temperature in mixed layer, while these studies also showed that the decadal variations of ocean mixed layer depth appear not in the northern and southern regions but in the central North Pacific (30N-40N, 180W-150W), and stronger in winter rather

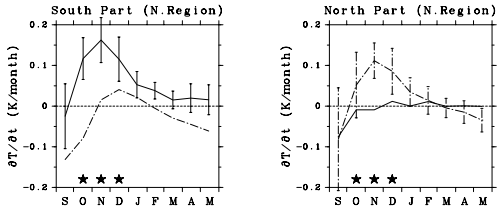

Fig. 7. Same as Fig.3, except for the composite values of the heat loss by meridional Ekman advection (solid line) and total heat flux at the sea surface (dashed-dotted line), dividing the northern region into the southern part (39N-43N) (left) and the northern part (45N-49N) (right).

	S. Region (Nov-Jan)	N. Region (Oct-Dec)	
		S. Part	N. Part
	Ekman	Ekman	Heat
Ratio	153.6	22.8	9.4
			(%)

Table 2. The ratio of the monthly composite value to the monthly climatology, for the heat loss by meridional Ekman advection ($E'/\overline{E}$), averaged during November - January in the southern region and averaged during October - December in the southern part of the northern region. And the ratio for the heat loss by total heat flux at the sea surface ($H'/\overline{H}$), averaged during October - December in the northern part of the northern region.

than in autumn. Considering these studies, the ratio of the standard deviation of decadal variation to the monthly climatology for ocean mixed layer depth, $h'/\overline{h}$, could be expected to only a few percents on spatial average in the northern and the southern region during autumn.

Table2 shows the ratio of the monthly composite value ($'$) to the monthly climatology ($\bar{}$) on spatial average for meridional Ekman temperature transport, $E'/\overline{E}$ ($E = -\tau_x/\rho_\circ f_\circ \overline{h}$), and total heat flux at the sea surface, $H'/\overline{H}$ ($H = Q_{net}/\rho_\circ c\overline{h}$). The ratio calculated for the heat loss by meridional Ekman advection ($E'/\overline{E}$) is significantly larger than the ratio expected for the ocean mixed layer depth ($h'/\overline{h}$) in the southern region, and also $E'/\overline{E}$ is larger in the southern part of the northern region. $E'/\overline{E} > h'/\overline{h}$ means that the decadal anomaly of the numerator is larger than that of the denominator in the $-\tau_x/\rho_\circ f_\circ h$. In other words, the increase (decrease) of the heat loss by meridional Ekman advection would not be canceled out by the increase (decrease) of water mass with the mixed layer deepening (shoaling).

In the northern part of the northern region, $H'/\overline{H}$ is not so large. However in this area, the year-to-year variations of the heat loss by Ekman heat divergence, which may be the main cause of the mixed layer depth changing through vertical mixing, are hardly correlated with the time coefficient for the first SVD mode (not shown). It implies that the anomalies of the mixed layer depth associated with the first SVD mode is smaller than that of the other areas, and may be smaller than the anomalies of total heat flux. Hence, total heat flux in this area as well as meridional Ekman advection in the other areas is still important for the maintenance of decadal SST anomalies, even if the decadal variations of the ocean mixed layer depth and the vertical mixing process exist.

6. CONCLUSIONS

Over the midlatitude North Pacific, the seasonal variations and the mechanism for the maintenance of decadal SST anomalies are discussed individually in the northern region (39N-49N, 165E-155W) and the southern region (25N-35N, 175E-145W). In the southern region the decadal SST anomaly is maintained only by meridional Ekman advection during November - January. On the other hand, in the northern region the decadal SST anomaly is maintained by the sum of the effect of total heat flux at the sea surface and the effect of meridional Ekman advection during October - December. The above results suggest that the mechanisms for the maintenance of decadal SST anomalies would be different between in the northern region and the southern region.

REFERENCES

Barsugli, J. J. and D. S. Battisti, 1998: The basic effects of atmosphere-ocean thermal coupling on midlatitude variability. *J. Atmos. Sci.*, **55**, 477-493.

Deser, C., M. A. Alexander and M. S. Timlin, 1996: Upper-ocean thermal variations in the North Pacific during 1970-1991. *J. Climate*, **9**, 1840-1855.

Miller, A. J., D. R. Cayan, T. P. Barnett, N. E. Graham and J. M. Oberhuber, 1994: Interdecadal variability of the Pacific ocean: Model response to observed heat flux and wind stress anomalies. *Clim. Dyn.*, **9**, 287-302.

Nakamura, H., G. Lin and T. Yamagata, 1997: Decadal climate variability in the North Pacific during the recent decades. *Bull. Amer. Meteor. Soc.*, **78**, 2215-2225.

Saravanan, R., 1998: Atmospheric low-frequency variability and its relationship to midlatitude SST variability: Studies using the NCAR climate system model. *J. Climate*, **11**, 1386-1404.